A mouse model provides evidence that genetic background modulates anemia and liver injury in erythropoietic protoporphyria.

Marie Abitbol, Florence Bernex, H. Puy, H. Jouault, J.C. Deybach, J.L. Guenet, Xavier Montagutelli

Am J Physiol Gastrointest Liver Physiol 288: G1208–G1216, 2005.
First published January 27, 2005; doi:10.1152/ajpgi.00505.2004.

A mouse model provides evidence that genetic background modulates anemia and liver injury in erythropoietic protoporphyria

Marie Abitbol,[1] Florence Bernex,[2] Hervé Puy,[3] Hélène Jouault,[4] Jean-Charles Deybach,[3] Jean-Louis Guénet,[1] and Xavier Montagutelli[1]

[1]*Unité de Génétique des Mammifères and URA 2579 CNRS, Institut Pasteur, Paris;* [2]*UMR 955 INRA-ENVA de Génétique Moléculaire et Cellulaire and UP d'Histologie et d'Anatomie Pathologique, Ecole Nationale Vétérinaire d'Alfort, Maisons-Alfort;* [3]*Centre Francais des Porphyries, INSERM U 656, Faculté X. Bichat, Hopital Louis Mourier, Colombes; and* [4]*INSERM U 492-Université Paris XII, Faculté de Médecine, Créteil, France*

Submitted 11 November 2004; accepted in final form 18 January 2005

Abitbol, Marie, Florence Bernex, Hervé Puy, Hélène Jouault, Jean-Charles Deybach, Jean-Louis Guénet, and Xavier Montagutelli. A mouse model provides evidence that genetic background modulates anemia and liver injury in erythropoietic protoporphyria. *Am J Physiol Gastrointest Liver Physiol* 288: G1208–G1216, 2005. First published January 27, 2005; doi:10.1152/ajpgi.00505.2004.—Erythropoietic protoporphyria is an inherited disorder of heme biosynthesis caused by partial ferrochelatase deficiency, resulting in protoporphyrin (PP) overproduction by erythrocytes. In humans, it is responsible for painful skin photosensitivity and, occasionally, liver failure due to accumulation of PP in the liver. The ferrochelatase deficiency mouse mutation is the best animal model available for human erythropoietic protoporphyria. The original description, based on mice with a BALB/cByJCrl genetic background, reported a disease resembling the severe form of the human disease, with anemia, jaundice, and liver failure. Using congenic strains, we investigated the effect of genetic background on the severity of the phenotype. Compared with BALB/cByJCrl, C57BL/6JCrl mice developed moderate but increasing anemia and intense liver accumulation of PP with severe hepatocyte damage and loss. Bile excretory function was not affected, and bilirubin remained low. Despite the highest PP concentration in erythrocytes, anemia was mild and there were few PP deposits in the liver in SJL/JOrlCrl homozygotes. Discriminant analysis using six hematologic and biochemical parameters showed that homozygotes of the three genetic backgrounds could be clustered in three well-separated groups. These three congenic strains provide strong evidence for independent genetic control of bone marrow contribution of PP overproduction to development of liver disease and biliary PP excretion. They provide a tool to investigate the physiological mechanisms involved in these phenotypic differences and to identify modifying genes.

protoporphyrin; bilirubin; chronic hepatitis; ferrochelatase; congenic strains

ERYTHROPOIETIC PROTOPORPHYRIA (EPP) is an inherited disease of heme synthesis caused by a partial deficiency of the mitochondrial enzyme ferrochelatase (FECH, EC 4.99.1.1), which catalyzes the insertion of ferrous iron into protoporphyrin (PP) IX (2, 5). Reduced FECH activity results in decreased synthesis of Hb in red blood cells (RBC) and accumulation of PP, which is hydrophobic and excreted in bile. PP is highly cytotoxic and induces tissue damage through reactions with free radicals, especially in the skin after light exposure (19). The disease is diagnosed in children who develop painful skin inflammation after short exposure to sunlight. In <5% of patients, it may progress to severe hepatobiliary disease and hepatic failure and may require liver transplantation (13). Patients show a range of phenotypic severity that is not strictly correlated with the nature of the mutation (12, 16, 32). However, recent data have shown reduced levels of FECH enzyme activity (15–30% of normal) due to the coinheritance of a null allele with a normal "low-expressed" allele in patients suffering from photodermatitis (9–11). Characterization of other genetic risk factors would be of major medical interest for early identification and care of patients with high probability of developing severe liver disease.

Two models of EPP have been reported in the mouse. An FECH exon 10 deletion was generated by gene targeting, resulting in a dominant-negative effect and embryonic lethality of homozygotes (20, 21). Heterozygotes show mild protoporphyria with no liver disease. The best animal model is an ethylnitrosourea-induced point mutation with fully recessive transmission, named FECH deficiency (symbol *Fech*^{m1Pas}, hereafter referred to as *fech*) (34). In the BALB/cByJCrl genetic background, to which the mutation was originally backcrossed, homozygotes show 5% residual FECH activity in liver and spleen and develop skin lesions, jaundice, and severe hepatic dysfunction with massive PP deposits. This model, which mimics the most severe hepatic forms of the disease, has been used to show that gene and cellular therapy may dramatically improve the condition (7, 8, 25, 29, 30). Influence of the genetic background on the hepatobiliary phenotype of the mutation was first suspected when *fech/fech* homozygous mice were produced with a compound background of 50% BALB/cByJCrl, 25% C57BL/6JCrl, and 25% SJL/JOrlCrl. In none of the 15 *fech/fech* mice was the serum intensely icteric, as in BALB/cByJCrl mice (unpublished data). Such background effects, where the phenotype of single-gene diseases is strongly influenced by genetic modifiers, have been reported, for example, in mouse models of hemochromatosis (6), cystic fibrosis (14, 15), and colorectal cancer (4).

We developed and characterized congenic strains on the BALB/cByJCrl, C57BL/6JCrl, and SJL/JOrlCrl inbred backgrounds to study how each of them modified the hematologic and hepatobiliary phenotypes of the *Fech*^{m1Pas} mutation. Results show that the impact of the mutation on erythropoiesis and hepatobiliary function is dramatically different between

Address for reprint requests and other correspondence: X. Montagutelli, Unité de Génétique des Mammifères, Institut Pasteur 25, rue du Docteur Roux, 75724 Paris cedex 15, France (E-mail: xmonta@pasteur.fr).

The costs of publication of this article were defrayed in part by the payment of page charges. The article must therefore be hereby marked "*advertisement*" in accordance with 18 U.S.C. Section 1734 solely to indicate this fact.

the three strains. This study provides evidence for independent genetic control of the contribution of PP overproduction by the bone marrow to development of liver disease and biliary PP excretion. These congenic strains offer a powerful tool to investigate pathophysiological processes underlying the three phenotypes and to identify modifying genes.

MATERIALS AND METHODS

Production and maintenance of congenic strains. Wild-type BALB/cByJCrl, C57BL/6JCrl, and SJL/JOrlCrl mice (BALB/c, C57BL/6, and SJL, respectively) were purchased from Charles River Laboratories (L'Arbresle, France). The original *Fech*^{m1Pas} mutation (34) had been previously backcrossed to the BALB/c inbred background for >10 generations. Congenic strains were developed similarly on C57BL/6 and SJL, with 10 generations of backcrossing to the recipient strain. At each backcross generation and in further crosses, mouse genotypes were identified by amplification of a genomic segment encompassing the point mutation that removes a *Bsp*HI restriction site. PCR products were produced and digested as previously described (3).

All mice were housed in the same animal room throughout the study. They received unlimited, autoclaved water and irradiated food pellets. According to standard husbandry procedure, they were maintained in filter-top cages with artificial fluorescent light, under a 12:12-h light-dark cycle. All animal procedures were performed in compliance with the French and European Regulations on Animal Welfare and with Public Health Service recommendations and were approved by the Institut Pasteur veterinary staff.

Two series of mice were bred and analyzed. The first series included six groups (+/+ and *fech/fech* for each congenic strain) of ten 3-mo-old mice (5 males and 5 females), which were analyzed for hematologic and biochemical parameters. In the second series, +/+ and *fech/fech* mice were analyzed at 6 wk, 3 mo, or 6 mo of age (5 males or females per group) for biochemical parameters and FECH activity. Heterozygous *+/fech* mice were also analyzed in the second series at 6 wk and 6 mo of age.

Hematology and biochemistry. Mice were anesthetized by intraperitoneal injection of xylazine-ketamine and weighed. Blood was collected by puncture of the orbital sinus. RBC, Hb, hematocrit (Hct), mean cell volume (MCV), and mean cell content of Hb (MCCH) were measured using a Vet'ABC counter (SCIL, Viernheim, Germany). Total serum bilirubin (TBil), serum alkaline phosphatase (ALP), and serum aminotransferases [aspartate and alanine aminotransferase (ASAT and ALAT)] were measured with a VetTest analyzer (IDEXX, Cergy-Pontoise, France). PP levels in RBC and stools were determined by a method adapted from Poulos and Lockwood (26). Liver and spleen FECH activities were determined by synthesis of mesoporphyrin-Zn, adapted from Li et al. (17). Final mesoporphyrin-Zn concentration was measured using a fluorometer (model RF540, Shimadzu, Kyoto, Japan) with 410-nm excitation and 580-nm detection.

RBC fluorescence was used to evaluate erythrocytic PP concentration and was measured by flow cytometry using a FACscan analyzer (Becton-Dickinson). Total blood was diluted 1:15 with 0.9% NaCl. Geometric mean of RBC fluorescence was measured using the FL3 channel. A 3-mo-old C57BL/6 +/+ mouse was used to calibrate the analyzer, and the value was subtracted from that of every mouse tested.

Histology. Necropsy and liver histology were performed on +/+, *+/fech*, and *fech/fech* mice at 6 wk and 6 mo of age in the three congenic strains (3 mice per group). Liver samples were fixed in Tellyesniczky-Fekete solution during 36 h and dehydrated in 70% ethanol (28). Sections (5 μm) from the paraffin-embedded samples were routinely stained with hematoxylin, eosin, and saffran to evaluate hepatic lesions. PP deposits were assessed by typical birefringence under polarized light.

Statistical analysis. One- and two-way ANOVA were performed with StatView F-4.1 software (Abacus Concepts, Berkeley, CA). Distribution of values was assessed for normality by comparison with a normal distribution with the same mean and standard deviation using a Kolmogorov-Smirnov test. To reach distribution normality, logarithmic transformation of biochemical parameters (RBC fluorescence, TBil, ALP, ASAT, and ALAT) was used for ANOVA. Whenever possible, nonparametric tests (Mann-Whitney for 2 groups and Kruskal-Wallis for 3 groups) were performed for these variables, but they resulted in little variation of P values compared with ANOVA.

Parameters for which the genetic background strongly modified the effect of the mutation were subjected to discriminant analysis (SPSS version 11.5.0) to reduce the number of variables that best describe the differences between mutant mice in the three genetic backgrounds. Given a set of independent variables, discriminant analysis attempts to find linear combinations of those variables that best separate the groups of cases. These combinations are called discriminant functions. The number of discriminant functions is the lower of the number of original variables and the number of groups less 1. For example, if the original variables are x_1, x_2, and x_3, the first discriminant function is $d_1 = a_{10} + a_{11}x_1 + a_{12}x_2 + a_{13}x_3$, where a_{ij} is the constant coefficient of the jth variable of the ith function. Because the original variables were measured on different scales, they were standardized (so that the mean is null and the variance = 1 for every variable across the population) to compare coefficients. Standardized a_{ij} coefficients with large absolute values correspond to variables with greater discriminating ability. Group centroids were determined as the point with the smallest total distance to each individual point of the group.

RESULTS

Congenic strain production and clinical features. Congenic strains were produced by ≥10 generations of backcrossing to the recipient strain. Therefore, the congenic segment transferred with the mutation is, on average, 20 cM long (24, 33), representing <1.5% of the genome. No other donor allele is likely to be found on any other chromosome.

In the BALB/c and C57BL/6 backgrounds, *fech/fech* homozygotes showed growth retardation compared with *+/fech* littermates at 3 wk of age and reduction of fertility in adults of both genders, which was milder in C57BL/6 than in BALB/c mice (data not shown). These features were not noticed on the SJL background or in *+/fech* mice of the three strains. Serum and urine were icteric in *fech/fech* homozygotes of the three backgrounds, but this characteristic was much more intense in BALB/c mice. Jaundice was visible on ears in young albino BALB/c and SJL homozygotes. No spontaneous photosensitivity lesions were observed under our husbandry conditions. Clinical observations suggested that the mutation had a more severe impact on the general condition in BALB/c and C57BL/6 than in SJL mice.

Strain differences at 3 mo of age define three variants of the disease. A first group of mice was analyzed at 3 mo of age, which corresponds to the age of a young adult mouse. Most of the parameters we investigated were modified by the mutation, as reported in the original description of the mutation (34). The most outstanding features observed in homozygotes, albeit with very significant variations across strains, were considerable increase in liver and spleen size and weight and decrease in Hb, Hct, MCV, and MCCH due to decreased Hb synthesis (Fig. 1). RBC fluorescence, used to estimate intraerythrocytic accumulation of PP, was increased, as was TBil, which correlated with the jaundice observed macroscopically. Serum con-

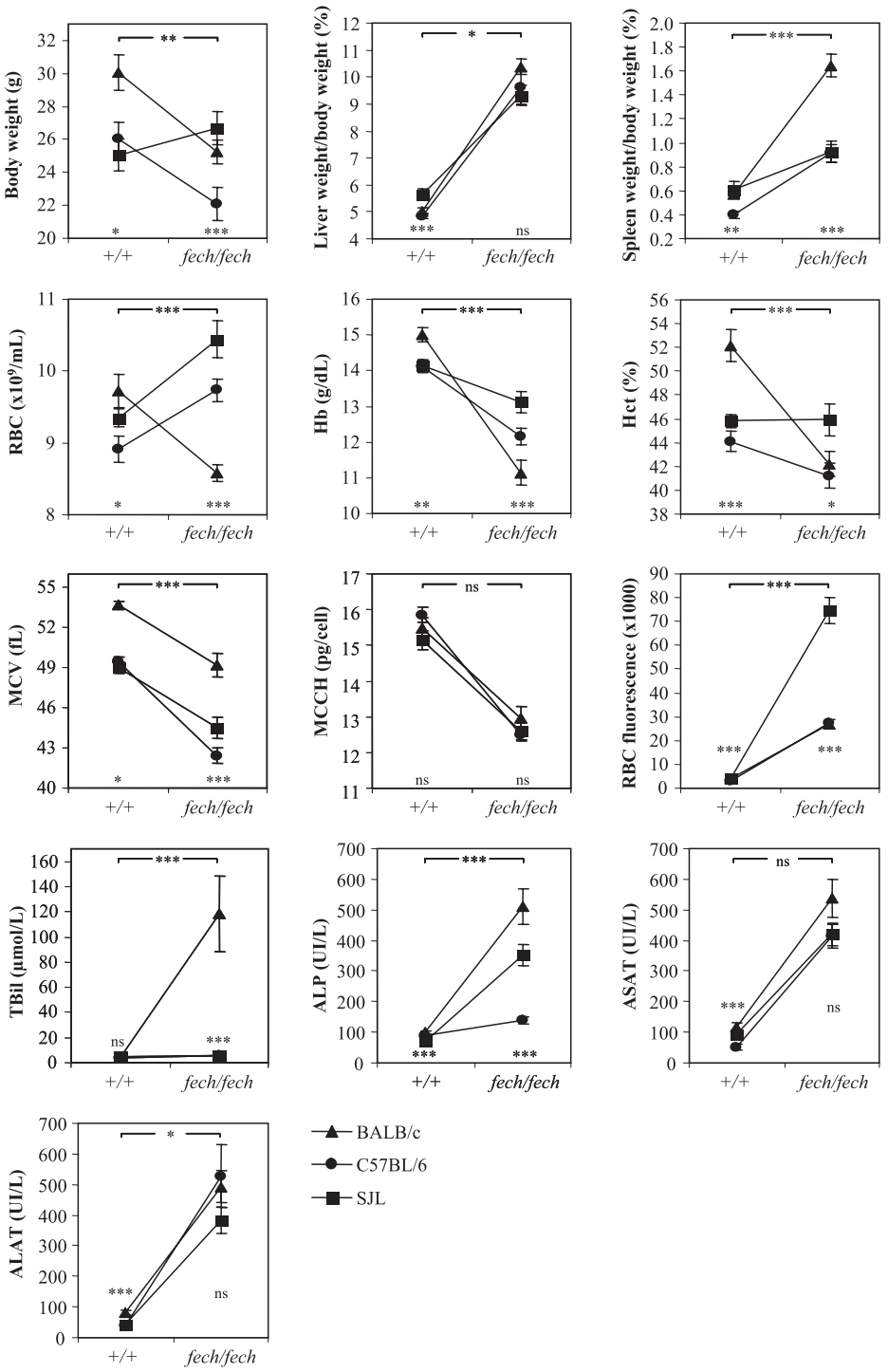

Fig. 1. Parameters measured in 3-mo-old +/+ and *fech/fech* mice in BALB/c, C57BL/6, and SJL mice (10 per group). RBC, red blood cell; MCV, mean cell volume; Hct, hematocrit; MCCH, mean cell content of Hb; TBil, total bilirubin; ALP, serum alkaline phosphatase; ALAT, alanine aminotransferase; ASAT, aspartate aminotransferase. Values are means ± SE. Asterisks above the *x*-axis indicate significance of the effect of genetic background on the phenotype of +/+ and *fech/fech* mice (1-way ANOVA). Asterisks at top of graphs indicate significance of the influence of genetic background on modifications of each parameter induced by the mutation, as measured by the interaction component in 2-way ANOVA, with genotype and strain as factors. NS, not significant. $*P < 0.05$; $**P < 0.01$; $***P < 0.001$.

centrations of enzymes that reflect hepatocyte (ASAT and ALAT) or biliary duct cell (ALP) damage were also elevated.

There were very significant differences in these variables across strains in wild-type mice of the three inbred strains, as revealed by the results of one-way ANOVA (Fig. 1). In particular, RBC count, Hb concentration, Hct, and MCV were highest in BALB/c +/+ mice. Other differences that were found to be significant (such as RBC fluorescence and liver enzymes) were not due to large variations of the means but to very small intragroup standard deviations. Similarly, highly significant differences were found for various parameters between *fech/fech* mice of the three backgrounds. However, more interesting than absolute values is the influence of the genetic background on the modifications of each variable induced by the mutation, as measured by the interaction component in two-way ANOVA (Fig. 1).

Despite the severe hepato- and splenomegaly observed in all *fech/fech* mice, resulting in abdomen enlargement, body weight was reduced in BALB/c and C57BL/6 homozygotes ($P < 0.0014$ and $P < 0.014$, respectively), correlating with de-

creased adipose tissue deposits observed at necropsy, consistent with altered general condition. By contrast, body weight was similar in SJL *fech/fech* mice and their wild-type littermates ($P > 0.2$).

The effect of the mutation on hematologic parameters was also influenced by the genetic background. Although BALB/c *fech/fech* mice showed the most dramatic reduction in all hematologic variables, RBC count increased significantly and Hb was significantly reduced in C57BL/6 and SJL homozygotes. In SJL *fech/fech* mice, increased RBC almost compensated for reduced MCCH, so that Hb was 93% that of +/+ mice. Similarly, TBil in *fech/fech* mice was much higher in BALB/c than in the two other congenic strains ($P < 0.0001$). There was a threefold higher increase of RBC fluorescence in SJL than in BALB/c or C57BL/6 mice ($P < 0.0001$). Aminotransferases were consistently increased across strains, whereas ALP levels were much higher in BALB/c and SJL than in C57BL/6 mice ($P < 0.0001$). Taken together, these results show that the FECH deficiency mutation did not induce the same features in the three congenic strains.

Discriminant function analysis. To investigate this point further, we performed discriminant analysis on *fech/fech* mice to show that the groups of mutant mice of the three congenic strains were clearly distinguishable and to identify combinations of variables that best separate these groups. Eight variables (RBC, Hb, MCV, RBC fluorescence, TBil, ALP, body weight, and spleen-to-body weight ratio) had been found by ANOVA to be highly significantly influenced by the genetic background in *fech/fech* mice, with $P < 0.001$. Body and organ weights are likely a far downstream consequence of the mutation and were, therefore, discarded. Because three groups were considered, two discriminant functions were calculated, each of which was a linear combination of the six variables. To avoid scale effects, variables were standardized so that function coefficients could be compared between variables. Scatter plot of all *fech/fech* mice according to the discriminant functions shows that mutant mice could clearly be separated into three nonoverlapping groups according to their background strain (Fig. 2). The separation along the *x*-axis (*function 1*) primarily involved MCV and, almost equally, RBC fluorescence, Hb, RBC, and TBil. *Function 2* essentially involved ALP, but also Hb and RBC fluorescence. When the same discriminant functions were applied to +/+ mice, SJL and C57BL/6 mice were largely overlapping and very close to the BALB/c mice (data not shown).

Strain differences influence disease progression. Another group of mice was analyzed at 6 wk, 3 mo, and 6 mo of age to study disease progression in the three congenic strains. Hematologic consequences of the mutation were apparent at 6 wk of age in the three genetic backgrounds. Few parameters significantly changed with age, despite variations in mean ratios, mostly because of intragroup heterogeneity. The differences between congenic strains observed at 3 mo were consistently confirmed (data not shown).

The consequences of the mutation on the liver observed in 3-mo-old mice generally increased in severity with age. Figure 3 shows the values of *fech/fech* mice at each time point for biochemical parameters. The influence of age on the effect of the mutation was tested statistically for each congenic strain as the interaction component in two-way ANOVA, with age and genotype (+/+ compared with *fech/fech*) as factors (Fig. 3).

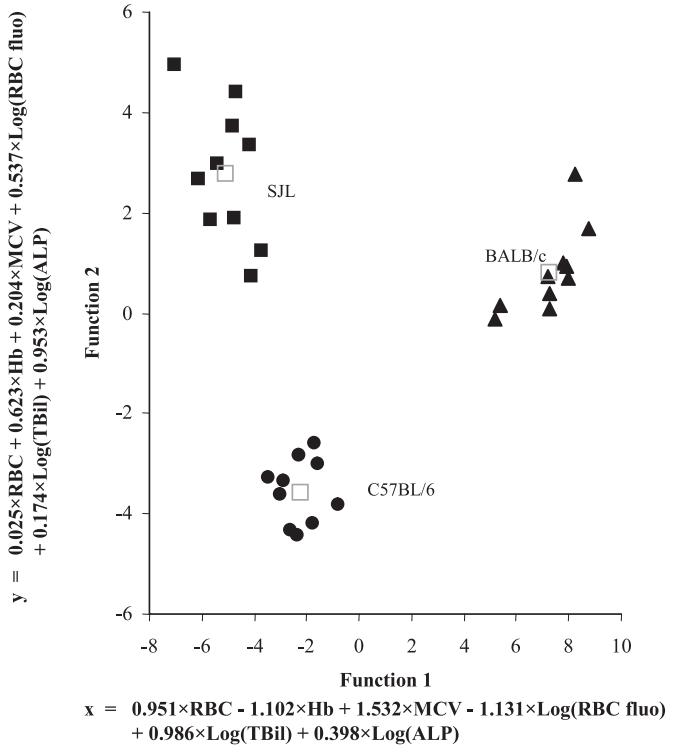

Fig. 2. Scatter plot of 3-mo-old *fech/fech* BALB/c, C57BL/6, and SJL mice (10 per strain) according to discriminant analysis. For each mouse, *x*- and *y*-axis coordinates are values calculated for the 1st and 2nd discriminant functions, respectively, using standardized variables. □, Group centroid, i.e., point with the smallest total distance to each individual point of the group.

TBil was much higher in BALB/c *fech/fech* than in the other strains at 3 mo of age and increased in adult mice (influence of age: $P < 0.006$), indicating severe alteration of liver excretory function. ALP also showed a highly significant increase with age ($P < 0.0001$), reflecting aggravation of biliary duct cell lesions. A progressive impairment of PP excretion through the bile was revealed by measurement of PP concentration in RBC and stools in the three age groups. Although no significant evolution with age was observed in C57BL/6 and SJL mice, BALB/c *fech/fech* mice showed a highly significant increase in the ratio of PP concentration in RBC to PP concentration in stools ($P < 0.0003$; Fig. 3), resulting mostly from a threefold decrease of PP in stools ($P < 0.0001$) between 6 wk and 6 mo of age.

Although high levels of aminotransferases were observed at 6 wk in *fech/fech* homozygotes across strains (>1,000 vs. 250–440 IU/l in +/+), the highest levels were found in adult C57BL/6 *fech/fech* mice (>2,000 IU/l in two of five 6-mo-old mice). The influence of age was not statistically significant because of large interindividual heterogeneity. ALP was normal up to 3 mo of age, as was TBil. At 6 mo, both were 3- and 17-fold higher, respectively, than in wild-type mice, suggesting progressive impairment of liver excretory function.

SJL *fech/fech* mice showed the least severe overall phenotype. By contrast, they showed the highest levels of RBC fluorescence at all ages. Liver function was moderately affected, with mild elevation of aminotransferases and ALP. TBil levels were 5- to 10-fold higher than in wild-type mice across age points.

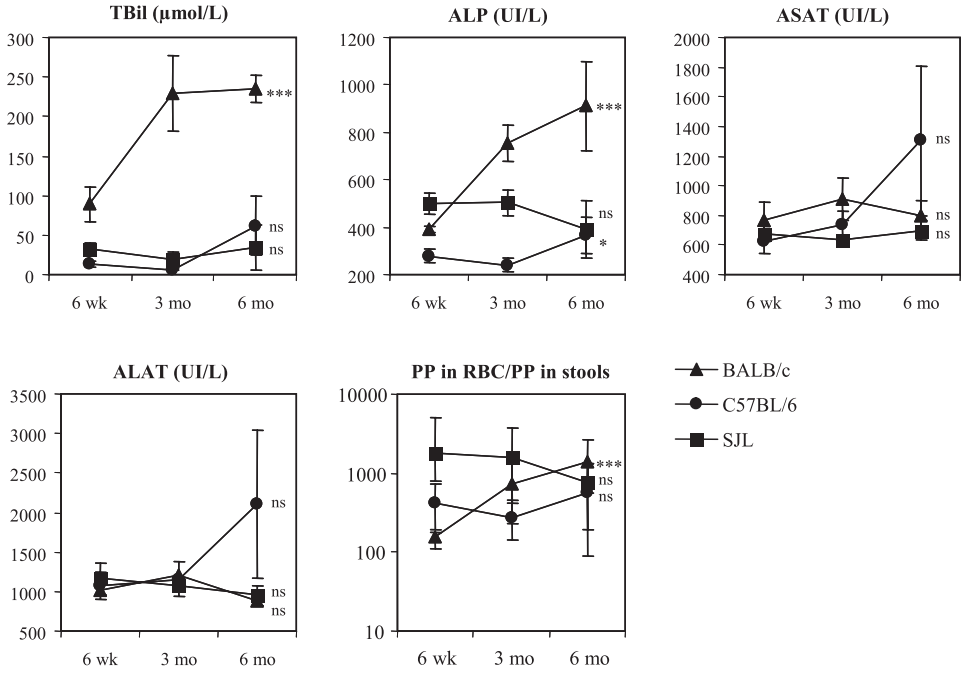

Fig. 3. Changes with time in selected variables in 6-wk, 3-mo-, and 6-mo-old BALB/c, C57BL/6, and SJL mice (5 per group). Values are means ± SE of *fech/fech* mice, except for the ratio of protoporphryin (PP) in RBC to PP in stools, where mean and range of individual values are given. Significance of the influence of age on the effect of the mutation, as measured by the interaction component in 2-way ANOVA with genotype (+/+ compared with *fech/fech*) and age as factors: $*P < 0.05$; $***P < 0.001$.

Heterozygotes were compared with wild-type mice at 6 wk and 6 mo of age in the three strains. The only significant observation was a transient anemia in 6-wk-old C57BL/6 *+/fech* mice, with a 18–19% reduction of Hb ($P < 0.0005$), Hct ($P < 0.006$), and MCV ($P < 0.0007$). All parameters returned to normal at 6 mo of age.

Strain differences influence FECH enzyme activity in liver and spleen. FECH activity was measured in liver and spleen of 6-wk- and 6-mo-old +/+, *+/fech*, and *fech/fech* mice (Fig. 4). Wild-type mice showed identical FECH activity across strains at 6 wk, but FECH activity was lower at 6 mo in C57BL/6 mice ($P < 0.013$). The original description of the $Fech^{m1Pas}$ mutation reported ~5 and 55% residual activity in homozygotes and heterozygotes, respectively. These results were confirmed in the liver across strains at 6 wk and in BALB/c mice at 6 mo. At 6 mo, C57BL/6 and SJL heterozygous mice showed higher activity than expected (both at 79%) compared with +/+. FECH activity (per g tissue) in 6-wk-old *+/fech* and *fech/fech* mice was significantly lower, in absolute values, in C57BL/6 than in BALB/c or SJL mice ($P < 0.009$ and $P < 0.0013$, respectively).

In the spleen, *fech/fech*-to-+/+ ratios were unexpectedly high: 14 and 19% in 6-mo-old SJL and BALB/c mice, respectively, and 24–39% in the other groups. Even more surprisingly, the expected 50–60% activity in heterozygotes was observed only in 6-mo-old BALB/c mice (54%); it was >74% in all other groups. We ruled out experimental artifacts, because samples were collected and treated randomly across groups, and intragroup standard deviations were small compared with intergroup differences. In terms of absolute values, splenic FECH activity was reduced in C57BL/6 *fech/fech* mice compared with BALB/c and SJL mice at 6 wk ($P < 0.0004$) and 6 mo ($P < 0.024$). These results show that genetic background may influence FECH activity in absolute values or

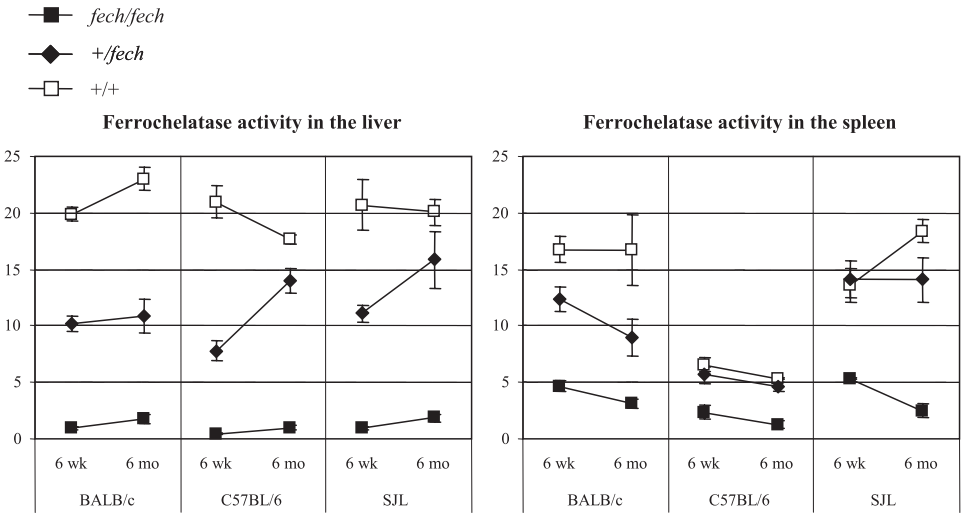

Fig. 4. Ferrochetalase (FECH) activity (nmol mesoporphyrin-Zn synthesized·mg protein^{-1}·h^{-1}) in liver and spleen in 6-wk- and 6-mo-old +/+, *+/fech*, and *fech/fech* mice (5 per group). Values are means ± SE.

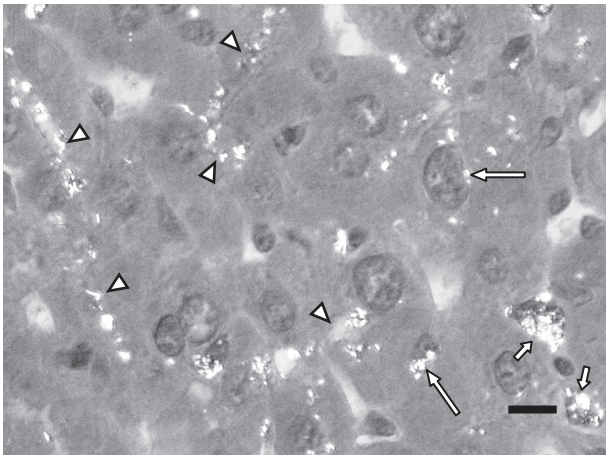

Fig. 5. Liver section of a 6-wk-old BALB/c *fech/fech* mouse under polarized light. PP nature of intrahepatic deposits was confirmed by typical red-to-yellow birefringence in hepatocytes (long arrows), bile canaliculi (arrowheads), and Küpffer cells (short arrows). In hepatocytes and within biliary canaliculi, crystals were small and isolated; in Küpffer cells, they were much larger, clustered, and mixed with bile. Scale bar, 10 μm.

in ratios. The most recurrent finding was a lower FECH activity in C57BL/6 mice, particularly in the spleen.

Strain differences influence liver pathology. In the three congenic strains, *fech/fech* mice showed moderate-to-severe hepatomegaly (Fig. 1) due to PP hepatocellular deposition and accumulation, cholestasis, and chronic hepatitis. Under polarized light, PP deposits were observed as small crystals characterized by red-to-yellow birefringence under polarized light in hepatocytes, bile canaliculi, and Küpffer cells (Fig. 5).

Cholestasis, characterized by bile retention within hepatic parenchyma, was noticed in enlarged hepatocytes, dilated bile canaliculi containing elongated green-brown bile plugs, and portal biliary ducts (Fig. 6). Küpffer cells phagocytosed and accumulated bile released from ruptured canaliculi. Bile accumulation was sometimes observed in various upstream bile ducts that had undergone proliferation. Chronic hepatitis consisted of fibrosis and inflammatory infiltrate, which were encountered at least in portal tracts and associated with isolated hepatocyte damage and loss and cell regeneration. The severity of these features was variable across strains (Table 1, Fig. 6).

At 6 wk, BALB/c *fech/fech* mice showed moderate PP deposits and accumulation in hepatocytes, canalicular ducts,

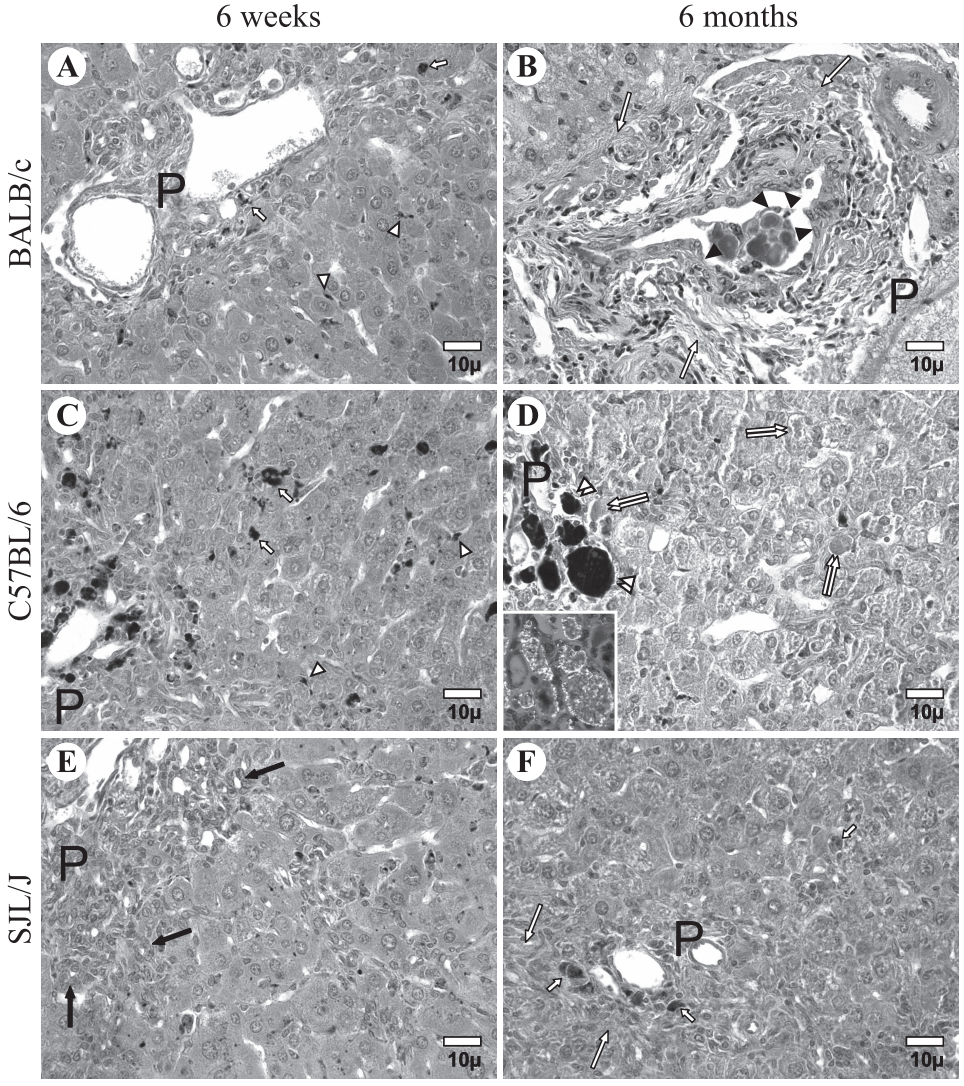

Fig. 6. Hematoxylin, eosin, and saffran staining of liver sections of 6-wk- and 6-mo-old *fech/fech* mice. P, portal tract. *A*: moderate accumulation of bile pigment in bile canaliculi (arrowheads) and Küpffer cells (short arrows) with moderate chronic hepatitis around portal tract. *B*: severe cholestasis in portal biliary duct due to mixed PP and bile plugs, responsible for epithelial duct cell damage and loss (arrowheads). Long arrows, severe chronic hepatitis with portal tract fibrosis. *C*: massive bile accumulation in bile canaliculi (arrowheads) and Küpffer cells (short arrows). *D*: enlarged portal macrophages filled with bile (double arrowheads) and PP, as revealed by birefringence under polarized light (*inset*). Double arrows, chronic hepatitis with severe cell damage and loss. *E*: mild cholestasis associated with moderate chronic hepatitis, with fibrosis and biliary duct hyperplasia (arrows). *F*: mild periportal fibrosis (long arrows) and bile accumulation in Küpffer cells (short arrows).

Table 1. *Lesions observed in 6-wk- and 6-mo-old fech/fech mice*

	BALB/c		C57BL/6		SJL/J	
Lesion Type	6 wk	6 mo	6 wk	6 mo	6 wk	6 mo
PP deposits	2	0–1	3	3	1	0–1
Cholestasis	2	3	2	2	1–2	0–1
Chronic hepatitis	2	3	3	3	1–2	1–2

0, None; 1, mild; 2, moderate; 3, severe. PP, protoporphyrin.

and macrophages (Fig. 5). PP deposits decreased with time, and PP crystals were only observed at 6 mo in rare macrophages. Cholestasis was then concentrated in macrophages and portal biliary ducts, the lining epithelial cells being damaged. Chronic hepatitis rose from moderate to severe, with portal fibrosis and biliary duct hyperplasia.

PP accumulation in C57BL/6 *fech/fech* mice was severe at 6 wk, with high concentrations in macrophages, in which PP deposits appeared as numerous agglomerated masses of variable size, and in the lumen of biliary canaliculi. Severe cholestasis and chronic hepatitis showed marked hepatocellular necrosis and regeneration.

PP accumulation was mild at 6 wk and nearly absent at 6 mo in SJL *fech/fech* mice. Cholestasis pigment accumulation was mild to moderate at 6 wk, and bile plugs were found later only in macrophages. Chronic hepatitis was mild to moderate.

In *+/fech* and +/+ mice, the liver was macroscopically normal in the three strains. Mild histological lesions were observed in 6-mo-old C57BL/6 *+/fech* mice, with PP deposits, associated with mild cholestasis and mild chronic hepatitis.

The histological features of the liver lesions in *+/fech* and *fech/fech* mice were different between strains with regard to *1*) PP deposition at 6 wk (mild in SJL, moderate in BALB/c, and severe in C57BL/6), decreasing with time (persistent only in rare macrophages in SJL and BALB/c and in numerous portal macrophages in C57BL/6), *2*) diffuse cholestasis at 6 wk (mild to moderate in SJL and moderate in BALB/c and C57BL/6), with bile plugs mostly found in Küpffer cells and macrophages at 6 mo, *3*) chronic hepatitis (mild to moderate in SJL and BALB/c and severe in C57BL/6), and *4*) evolution of lesions between 6 wk and 6 mo (decreasing PP deposition and cholestasis in SJL and constant or aggravating in BALB/c and C57BL/6; Fig. 6, Table 1).

These observations emphasize strain differences in PP deposits and clearance with age, pigment macrophage accumulation, and necrosis and regeneration of biliary epithelial cells and hepatocytes.

DISCUSSION

EPP is one of the inherited disorders originally considered as being transmitted in a Mendelian fashion, in which additional genetic factors must be involved to explain phenotypic diversity. The major complication of EPP, which affects <5% of patients, remains the development of severe hepatobiliary dysfunction progressing to liver failure, which is fatal in the absence of liver transplantation.

The FECH deficiency mouse mutation has proven to be a valuable animal model for EPP studies. Gene (8, 25, 29, 30) and cellular (7) therapy experiments showed that correcting the FECH deficiency results in very significant improvement of hematopoietic and liver functions. Recent work has focused on liver pathology, which is a key feature of this model (18). However, when this mutation is maintained on the BALB/c genetic background, it mimics the most severe hepatic forms of the human disease. Because liver pathology and PP accumulations in RBC develop in the 1st wk, it is difficult to establish the respective implications, in liver PP loading, of PP release from degraded RBC and of PP synthesis by the liver. This study started with the unexpectedly mild jaundice observed in *fech/fech* mice resulting from an F2 cross between the mutant strain and (C57BL/6 × SJL)F1 mice, which suggested that the phenotype of the *fech* mutation is strongly influenced by the genetic background.

Most studies published on genetic background effects have focused on the mapping of genetic modifiers in segregating crosses between two inbred strains. Although such studies point to putative genomic locations, the phenotypes are neither fixed nor reproducible, because each F2 mouse is genetically unique. As a consequence and because each mouse provides a limited source of material, pathophysiological mechanisms responsible for phenotypic differences between individuals cannot be investigated in depth. In addition, the designated genomic regions are large, and gene identification requires substantial additional work. In contrast, congenic strains are genetically and phenotypically stable populations that can be thoroughly characterized to precisely delineate phenotypic differences, understand their underlying mechanisms, and provide

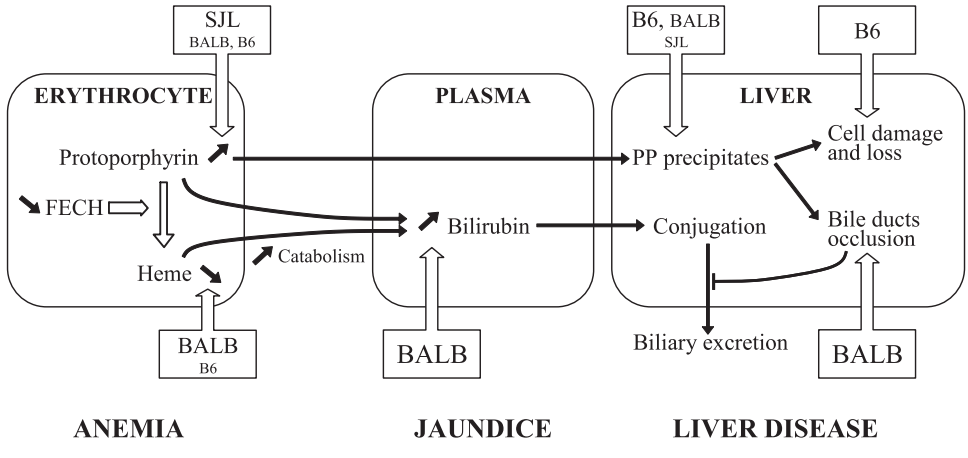

Fig. 7. Model of pathophysiology of erythropoietic protoporphyrin (EPP). Boxed arrows indicate congenic strains where the phenotype is observed, with intensity reflected by font size. SJL mice are characterized by pronounced PP accumulation in RBC but reduced PP deposition in the liver. C57BL/6 (B6) show marked intracellular PP deposits, associated with cell damage and loss, and chronic hepatitis. BALB/c mice develop anemia and show obstruction of biliary ducts by PP deposits, impairing bilirubin fecal excretion.

stable and reproducible animal models for a human disease (1, 6, 27, 31).

We have developed congenic strains by introducing the FECH deficiency mutation in the C57BL/6 and SJL inbred backgrounds. Our results demonstrate that the same mutation results in very different forms of the disease in the three strains. BALB/c *fech/fech* mice develop hypochromic and microcytic anemia, with 25% reduction of Hb and 21% decrease of Hct at 6 wk, which does not improve with age. PP overproduction by RBC results in moderate pigment deposits in the liver. However, impairment of the liver excretory function is rapid and profound, as shown by elevated TBil and ALP levels and by progressive decrease in fecal PP excretion. C57BL/6 *fech/fech* mice show moderate anemia, with 19% Hb reduction and 15% Hct decrease at 3 mo. This strain shows by far the most pronounced liver accumulation of pigment, with very large deposits in hepatocyte cytoplasm, Küpffer cells, bile canaliculi, and periportal bile ducts. This was characterized by increasing levels of aminotransferases and by chronic hepatitis with aggravating hepatocellular damage and loss. However, the liver excretory function was almost unaffected, with high PP fecal excretion and ALP and TBil concentrations moderately increased only in 6-mo-old mice. SJL *fech/fech* mice were undoubtedly the least affected, with discrete hypochromic anemia and mild liver lesions. These mice had the highest PP concentration in RBC but the mildest PP loading in the liver.

The three forms of EPP described here are contrasted by the panel of parameters measured. Differences are so obvious that six clinical parameters were sufficient to unequivocally assign every mutant mouse to its proper group by discriminant analysis, a method that aims at reducing the number of quantitative variables necessary to describe individuals without loss of much information. The same functions did not discriminate wild-type mice of the three strains, suggesting that the classification of *fech/fech* mice did not result from differences intrinsic to the background strains, but from the different effects of the mutation in the three congenic strains.

The pathophysiological events associated with EPP can be summarized as shown in Fig. 7. It is generally accepted that *1*) FECH deficiency results in reduced Hb synthesis and intraerythrocytic PP accumulation, *2*) PP released in the plasma is taken up by the liver, where it precipitates because of its high hydrophobicity, *3*) PP deposits in hepatocytes cause cell damage and loss, resulting in fibrosis and regeneration, and *4*) PP crystals in biliary ducts impair excretion of bilirubin-rich bile (2). However, this general model is challenged by our observations (Fig. 7). Indeed, the most compelling result from this study is the absence of correlation between Hb deficit, PP accumulation in RBC, PP deposits in the liver, hepatocellular damage, and jaundice. Although all strains displayed a similar decrease in MCCH at 3 mo (Fig. 1), accumulation of PP in RBC was 3.4-fold higher in SJL than in C57BL/6 mice. However, liver PP deposits were considerably more important in C57BL/6 than in SJL mice.

Our data, based on genetically defined congenic strains, provide evidence for independent genetic control of PP accumulation in RBC and of PP clearance and accumulation by the liver. The high PP concentration in the RBC of SJL *fech/fech* mice may result from higher activity of enzymes upstream FECH, which influences the amount of PP produced as a final metabolite, or from reduced release of PP by RBC. A potential modifying gene could also be the *Abcg2* transporter, which was recently shown to play a role in regulating PP IX levels during erythroid differentiation (35).

Our histological observations suggest that the genetic background may influence the preferential site of PP deposition in the liver. Although overall PP accumulation in the liver was lower in BALB/c than in C57BL/6 mice, BALB/c mice developed bile excretory failure with increased ALP and TBil due to bile duct obstruction with PP precipitates. On the contrary, C57BL/6 mice showed marked intracellular PP deposits in the liver, associated with hepatocyte damage and loss and chronic hepatitis. Recently, using the congenic strains described here, Navarro et al. (23) reported increased mitochondrial respiratory chain enzyme activities in BALB/c and SJL *fech/fech* compared with +/+ mice. Such an increase, which could play a protective role against the cytotoxic effects of PP, was not observed in C57BL/6 mice.

The direct role of the level of FECH activity remains unclear. The three congenic strains did not significantly differ in liver FECH activity. The puzzling data obtained for the spleen could be due to different cellular composition between strains and genotypes.

The three congenic strains provide unparalleled material to unravel the pathophysiological mechanisms and identify genes that control the phenotypic differences reported here. However, demonstrating the molecular nature of genes underlying quantitative modifications of a phenotype remains a long and tedious process that requires additional crosses and congenic strains.

ACKNOWLEDGMENTS

We are grateful to Franck Bourgade for expert technical assistance in producing congenic strains. We thank Vasco Da Silva and Sylvie Simonin for technical help with FECH activity measurements, Colette Elbaz for technical assistance with histology, Jean-Jacques Fontaine for polarized light photographs, and Sylvain Bellier, Laurent Gouya, and Carole Beaumont for fruitful scientific discussions.

GRANTS

This study was supported through a fellowship of the Fédération des Maladies Orphelines (to M. Abitbol) and by a grant from GIS-Maladies Rares 2004/2005 Research Network on Rare Disorders.

REFERENCES

1. **Al-Saktawi K, McLaughlin M, Klugmann M, Schneider A, Barrie JA, McCulloch MC, Montague P, Kirkham D, Nave KA, and Griffiths IR.** Genetic background determines phenotypic severity of the *Plp rumpshaker* mutation. *J Neurosci Res* 72: 12–24, 2003.
2. **Anderson KE, Sassa S, Bishop DF, and Desnick RJ.** The porphyrias. In: *The Metabolic Basis of Inherited Diseases* (8th ed.), edited by Scriver CR, Beaudet AL, Sly WS, and Valle D. New York: McGraw-Hill, 2001, p. 2991–3062.
3. **Boulechfar S, Lamoril J, Montagutelli X, Guénet JL, Deybach JC, Nordmann Y, Dailey H, Grandchamp B, and de Verneuil H.** Ferrochelatase structural mutant (*Fech^{m1Pas}*) in the house mouse. *Genomics* 16: 645–648, 1993.
4. **Cormier RT, Hong KH, Halberg RB, Hawkins TL, Richardson P, Mulherkar R, Dove WF, and Lander ES.** Secretory phospholipase Pla2g2a confers resistance to intestinal tumorigenesis. *Nat Genet* 17: 88–91, 1997.
5. **Ferreira GC.** Ferrochelatase. *Int J Biochem Cell Biol* 31: 995–1000, 1999.
6. **Fleming RE, Holden CC, Tomatsu S, Waheed A, Brunt EM, Britton RS, Bacon BR, Roopenian DC, and Sly WS.** Mouse strain differences determine severity of iron accumulation in Hfe knockout model of hereditary hemochromatosis. *Proc Natl Acad Sci USA* 98: 2707–2711, 2001.

7. **Fontanellas A, Mazurier F, Landry M, Taine L, Morel C, Larou M, Daniel JY, Montagutelli X, de Salamanca RE, and de Verneuil H.** Reversion of hepatobiliary alterations by bone marrow transplantation in a murine model of erythropoietic protoporphyria. *Hepatology* 32: 73–81, 2000.
8. **Fontanellas A, Mendez M, Mazurier F, Cario-Andre M, Navarro S, Ged C, Taine L, Géronimi F, Richard E, Moreau-Gaudry F, EdS R, and de Verneuil H.** Successful therapeutic effect in a mouse model of erythropoietic protoporphyria by partial genetic correction and fluorescence-based selection of hematopoietic cells. *Gene Ther* 8: 618–626, 2001.
9. **Gouya L, Deybach JC, Lamoril J, da Silva V, Beaumont C, Grandchamp B, and Nordmann Y.** Modulation of the phenotype in dominant erythropoietic protoporphyria by a low expression of the normal ferrochelatase allele. *Am J Hum Genet* 58: 292–299, 1996.
10. **Gouya L, Puy H, Lamoril J, da Silva V, Grandchamp B, Nordmann Y, and Deybach JC.** Inheritance in erythropoietic protoporphyria: a common wild-type ferrochelatase allelic variant with low expression accounts for clinical manifestation. *Blood* 93: 2105–2110, 1999.
11. **Gouya L, Puy H, Robreau AM, Bourgeois M, Lamoril J, da Silva V, Grandchamp B, and Deybach JC.** The penetrance of dominant erythropoietic protoporphyria is modulated by expression of wildtype FECH. *Nat Genet* 30: 27–28, 2002.
12. **Gouya L, Schneider-Yin X, Rufenacht U, Herrero C, Lecha M, Mascaro JM, Puy H, Deybach JC, and Minder EI.** Mutations in the ferrochelatase gene of four Spanish patients with erythropoietic protoporphyria. *J Invest Dermatol* 111: 406–409, 1998.
13. **Gross U, Frank M, and Doss MO.** Hepatic complications of erythropoietic protoporphyria. *Photodermatol Photoimmunol Photomed* 14: 52–57, 1998.
14. **Haston CK, McKerlie C, Newbigging S, Corey M, Rozmahel R, and Tsui LC.** Detection of modifier loci influencing the lung phenotype of cystic fibrosis knockout mice. *Mamm Genome* 13: 605–613, 2002.
15. **Haston CK and Tsui LC.** Loci of intestinal distress in cystic fibrosis knockout mice. *Physiol Genomics* 12: 79–84, 2003.
16. **Henriksson M, Timonen K, Mustajoki P, Pihlaja H, Tenhunen R, Peltonen L, and Kauppinen R.** Four novel mutations in the ferrochelatase gene among erythropoietic protoporphyria patients. *J Invest Dermatol* 106: 346–350, 1996.
17. **Li FM, Lim CK, and Peters J.** An HPLC assay for rat liver ferrochelatase activity. *Biomed Chromatogr* 2: 164–168, 1987.
18. **Libbrecht L, Meerman L, Kuipers F, Roskams T, Desmet V, and Jansen P.** Liver pathology and hepatocarcinogenesis in a long-term mouse model of erythropoietic protoporphyria. *J Pathol* 199: 191–200, 2003.
19. **Lim HW.** Pathophysiology of cutaneous lesions in porphyrias. *Semin Hematol* 26: 114–119, 1989.
20. **Magness ST and Brenner DA.** Targeted disruption of the mouse ferrochelatase gene producing an exon 10 deletion. *Biochim Biophys Acta* 1453: 161–174, 1999.
21. **Magness ST, Maeda N, and Brenner DA.** An exon 10 deletion in the mouse ferrochelatase gene has a dominant-negative effect and causes mild protoporphyria. *Blood* 100: 1470–1477, 2002.
22. **Meerman L, Koopen NR, Bloks V, van Goor H, Havinga R, Wolthers BG, Kramer W, Stengelin S, Muller M, Kuipers F, and Jansen PLM.** Biliary fibrosis associated with altered bile composition in a mouse model of erythropoietic protoporphyria. *Gastroenterology* 117: 696–705, 1999.
23. **Navarro S, del Hoyo P, Campos Y, Abitbol M, Morán-Jiménez MJ, García-Bravo M, Pilar Ochoa P, Grau M, Montagutelli X, Frank J, Garesse R, Arenas J, Enríquez de Salamanca R, and Fontanellas A.** Increased mitochondrial respiratory chain enzyme activities correlate with minor extent of liver damage in mice suffering from erythropoietic protoporphyria. *Exp Dermatol* 14: 26–33, 2005.
24. **Panthier JJ, Montagutelli X and Guénet JL** *Génétique de la souris*. Paris: Belin, 2003.
25. **Pawliuk R, Bachelot T, Wise RJ, Mathews-Roth MM, and Leboulch P.** Long-term cure of the photosensitivity of murine erythropoietic protoporphyria by preselective gene therapy. *Nat Med* 5: 768–773, 1999.
26. **Poulos V and Lockwood WH.** A rapid method for estimating red blood cell porphyrin. *Int J Biochem* 12: 1049–1050, 1980.
27. **Qiu J, Ogus S, Mounzih K, Ewart-Toland A, and Chehab FF.** Leptin-deficient mice backcrossed to the BALB/cJ genetic background have reduced adiposity, enhanced fertility, normal body temperature, and severe diabetes. *Endocrinology* 142: 3421–3425, 2001.
28. **Relyea MJ, Miller J, Sundberg JP, and Boggess D.** Necropsy methods for laboratory mice: biological characterization of a new mutation. In: *Systematic Approach to Evaluation of Mouse Mutations*, edited by Sundberg JP and Boggess D. Boca Raton, FL: CRC, 2000, p. 57–89.
29. **Richard E, Mendez M, Mazurier F, Morel C, Costet P, Xia P, Fontanellas A, Geronimi F, Cario-Andre M, Taine L, Ged C, Malik P, de Verneuil H, and Moreau-Gaudry F.** Gene therapy of a mouse model of protoporphyria with a self-inactivating erythroid-specific lentiviral vector without preselection. *Mol Ther* 4: 331–338, 2001.
30. **Richard E, Robert E, Cario-Andre M, Ged C, Geronimi F, Gerson SL, de Verneuil H, and Moreau-Gaudry F.** Hematopoietic stem cell gene therapy of murine protoporphyria by methylguanine-DNA-methyltransferase-mediated in vivo drug selection. *Gene Ther* 11: 1638–1647, 2004.
31. **Rogner UC and Avner PA.** Congenic mice: cutting tools for complex immune disorders. *Nat Rev Immunol* 3: 243–252, 2003.
32. **Rufenacht UB, Gouya L, Schneider-Yin X, Puy H, Schafer BW, Aquaron R, Nordmann Y, Minder EI, and Deybach JC.** Systematic analysis of molecular defects in the ferrochelatase gene from patients with erythropoietic protoporphyria. *Am J Hum Genet* 62: 1341–1352, 1998.
33. **Silver LM.** *Mouse Genetics*. Oxford, UK: Oxford University Press, 1995.
34. **Tutois S, Montagutelli X, Da Silva V, Jouault H, Rouyer-Fessard P, Leroy-Viard K, Guénet JL, Nordmann Y, Beuzard Y, and Deybach JC.** Erythropoietic protoporphyria in the house mouse—a recessive inherited ferrochelatase deficiency with anemia, photosensitivity, and liver-disease. *J Clin Invest* 88: 1730–1736, 1991.
35. **Zhou S, Zong Y, Ney PA, Nair G, Stewart CF, and Sorrentino BP.** Increased expression of the Abcg2 transporter during erythroid maturation plays a role in decreasing cellular protoporphyrin IX levels. *Blood* 105: 2571–2576, 2005.